Fusion Engineering and Design xxx (xxxx) xxx–xxx

Contents lists available at ScienceDirect

Fusion Engineering and Design

journal homepage: www.elsevier.com/locate/fusengdes

Optimization of TE_{11}/TE_{04} mode converters for the cold test of a 250 GHz CARM source

G.L. Ravera[a,*], S. Ceccuzzi[a], G. Dattoli[a], E. Di Palma[a], A. Doria[a], G.P. Gallerano[a], E. Giovenale[a], F. Mirizzi[b], G. Schettini[c], I. Spassovsky[a], A.A. Tuccillo[a], the ENEA CARM Task Force

[a] ENEA, Fusion and Nuclear Safety Departement, C. R. Frascati, Via E. Fermi 45, 00044, Roma, Italy
[b] Consorzio CREATE, Via Claudio 21, I-80125, Napoli, Italy
[c] "Roma Tre" University, Department of Engineering, Via Vito Volterra 62, 00146 Roma, Italy

ARTICLE INFO

Keywords:
ECRH
DEMO
CARM

ABSTRACT

Electron Cyclotron Resonance Heating (ECRH) systems in future fusion devices, like the DEMO-nstration reactor, foresee an operational frequency in the range 230–280 GHz to match the plasma characteristics. Cyclotron Auto Resonance Masers (CARMs) could represent an alternative to gyrotrons as effective source of mm and sub-mm waves and the project of a 250 GHz, 0.5 MW CARM has been undertaken at ENEA. Mode converters from the TE_{10} in WR3 rectangular waveguide to the operational mode (TE_{53}) are required to perform the RF cold test of Bragg reflectors and cavities. In this paper an improved and feasible structure for the TE_{11} to TE_{04} conversion, in oversized circular waveguides, using only two transitions with profile and radius optimized in order to obtain high efficiencies and sufficient bandwidth, has been designed and the simulation results are presented. The first transition is a TE_{11}/TE_{01} serpentine mode converter in circular waveguide (efficiency of 95%) with average radius of 1.48 mm and an appropriate number of geometrical periods. The second one, a TE_{01}/TE_{04} rippled wall mode converter with efficiency of 97%, consists of a single conversion section with an average radius of 3 mm and sixteen sinusoidal periods instead of three conversion sections (TE_{01}/TE_{02}, TE_{02}/TE_{03}, TE_{03}/TE_{04}) in cascade, thus reducing the complexity and the length of the full transition chain.

1. Introduction

Nowadays efficient high-power continuous-wave (CW) sources of coherent mm-wave radiation cannot meet the challenging future demands that mostly come from diagnostic as well as heating and current drive systems in thermonuclear fusion research [1]. In parallel with gyrotron development other source concepts like the Cyclotron Auto-Resonance Maser (CARM) [2], are theoretically promising for mm waves. In this frame a research and development program has been undertaken at ENEA Frascati Research Center, aimed at realizing a microwave tube based on a 250 GHz CARM oscillator [3], characterized by a high value of the frequency Doppler up-shift allowing a consistent reduction of the static magnetic field in the interaction cavity. Several problems of mode competitions [4] have required an intensive activity to optimize the design parameters. Despite that our device will operate with the TE_{53} mode in a oversized cylindrical cavity with a radius of 7.5 mm delimited by bragg reflectors, the excitation of spurious modes can be kept under control by operating with an electron beam having a velocity spread lower than 0.5% and using slotted cavity to limit the amplitude of the modes with low starting current. The RF cold test, performed using a vector analyser with frequency extension modules in order to operate in the WR3 band (220–325 GHz), requires the design of mode converters able to transform the fundamental mode in rectangular waveguide to the TE_{53} operational mode. In the preliminary phase of the project the TE_{82} mode has been chosen as operational mode and two types of conversion chains [5] have been carefully analysed. Subsequently the TE_{53} mode has been preferred because its maximum electric field on the cross section, closer to the center of the cavity, allows strong interaction with the electron beam and few problems of mode competition. With the new operational mode in order to improve the conversion efficiency a different approach [6] for the whole conversion chain (TE_{11} to TE_{53} in circular waveguide) has been investigated using a sequence of several transitions (one serpentine and four rippled wall mode converters). While the RF components to transform the TE_{01} in WR3 rectangular waveguide to a linear polarization of the TE_{11} are already available, in [6] the TE_{04} to TE_{53} mode converter design has been already described and the TE_{01} to TE_{04} transition, made by four mode converters and three circular tapers,

* Corresponding author.
E-mail address: gianluca.ravera@enea.it (G.L. Ravera).

https://doi.org/10.1016/j.fusengdes.2019.01.069
Received 3 October 2018; Received in revised form 3 December 2018; Accepted 11 January 2019

from an implementation point of view, is very complicated and has a considerable length. In this paper a simplified solution for the TE_{11} to TE_{04} transition has been reported using only two mode converters: a TE_{11}/TE_{01} serpentine mode converter [7] with radius 1.48 mm and a TE_{01}/TE_{04} rippled wall mode converter [8] with radius 3 mm connected by a circular taper adopting profiles of the radius as simple as to make feasible RF components at 250 GHz. Rippled Wall and Serpentine mode converters perform a complete conversion between the desired modes in a oversized circular waveguides respectively using a small perturbations of the radius with suitable profile, or a bending of the centre line of radius with axial periodicity approximately equal to the beat wavelength ($\lambda_b = 2\pi/(\beta_m-\beta_n)$) between the two interacting modes, which wavenumbers are β_m and β_n. The construction requires a mechanical accuracy better than 2 ± μm. Copper electroforming and Computer Numerically Controlled (CNC) milling allowing to reach dimensional tolerances up to 1 mμ and surface roughness comparable to the skin depth of the copper at f = 250 GHz, make possible the fabrication of the prototypes. A first validation of the simulation tools at such a high frequency will be carried out through the construction of a short Bragg reflectors [9] with an average radius of 7.5 mm during the current year by an Italian Company. The available computational resources allow the simulation of one transition of the chain at a time with all our calculation codes (CST-MS, HFSS and in-house codes). In Fig. 1 the whole sequence from WR3 rectangular waveguide to the circular waveguide is shown.

2. TE_{11}/TE_{01} serpentine mode converter

The TE_{11}/TE_{01} conversion, between two modes which azimuthal indexes differ only of one, can be performed by a Serpentine mode converter in circular waveguide. In CST-MS selecting in input the first linear polarization of the TE_{11}, the cross section, as shown in the CST model of Fig. 2, maintains a constant radius (r1) and undergoes a periodical bending of the central line along only the x axis (plane of curvature perpendicular to the polarization of the TE_{11} mode).

The analytical surface used to construct the CST-MS model is given by the following expressions:

$$x(u, v) = r1 + a*\sin(2*\frac{\pi}{bc}*v))*\cos(u))*\cos(u) \quad (1)$$

$$y(u, v) = r1*\sin(u) \quad (2)$$

where u = 0-2*π is the azimuthal angle, v = 0-L with L = N*bc the length of the converter (bc geometrical period and N number of geometrical periods) and *a* is the ripple amplitude. The average radius of r1 = 1.48 mm limits at 28 the number of propagation modes at f = 250 GHz and the simulations are executed without inserting symmetry planes. Results obtained by CST_MS are indicated in Fig. 3 versus the frequency. Indexes outside brackets of S parameters represent the input (n.1) or the output (n.2) port while the indexes in brackets are the order of the modes (TE_{11} is the 1 st and TE_{01} the 6th). The power reflection of the input mode isn't indicated because with small ripple amplitude its level is always under -30 dB. The maximum values of S2(6),1(1), whose square corresponds to the efficiency of the converter, have been achieved at f = 250 GHz, for values of N in the range 7–14, properly choosing bc and a, and using aluminum around the RF structure except only for the blue curve (N = 11) where a perfect electric conducting (PEC) walls has been taken in consideration. The beat wavelength (λb) of 11.73 mm between the two mode interacting at f = 250 GHz is slight shorter than the optimized geometrical period (bc). In the Serpentine mode converter increasing N, the condition of maximum conversion at f = 250 GHz on the desired mode have been achieved reducing both bc and a. Comparing all the solutions N = 11 (a = 0.088 and bc = 11.8) has been chosen because presents a maximum efficiency of about 95%, including also the RF losses, and a sufficient bandwidth. A further reduction of the bandwidth and a greater length of the RF component is obtained for higher N while lower efficiencies are produced for N > 11. The difference between the values of S2(6),1(1) of about 0.14 dB for N = 11 deduced with and without aluminum, corresponds to the ohmic losses of the RF component.

The content of the more important spurious modes for N = 11 is shown in Fig. 4.

A single polarization of TE_{12} has the highest amplitude and at

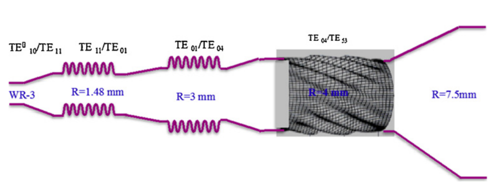

Fig. 1. Conversion chain with all mode converters and tapers.

Fig. 2. CST-MS model of the serpent-like TE_{11}-TE01 mode converter with radius of 1.48 mm.

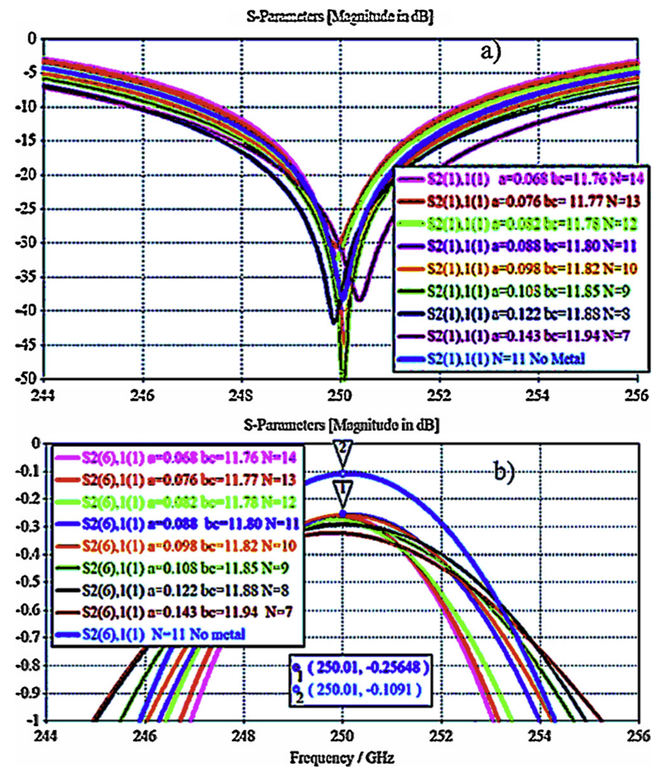

Fig. 3. CST_MS simulation results expressed in dB for N between 7 and 14 and for the PEC Serpentine converter with N = 11: a) Transmission in output of the TE_{11}, b) Conversion efficiency (dB).

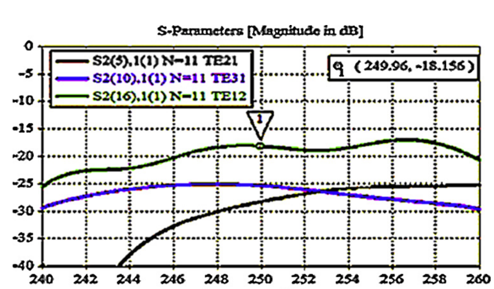

Fig. 4. Undesired modes with the highest amplitude at the output for N = 11.

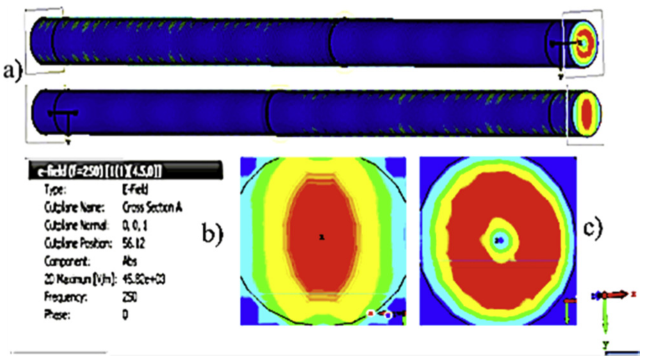

Fig. 5. Pattern of the electric field at f = 250 GHz with N = 11: a) along the Serpentine mode converter, b) Input port, c) Output port.

f = 250 GHz the content is under the 2%. Assuming the bandwidth as the interval between frequencies with 90% of efficiency its value is about 4 GHz. Significant is the pattern of the electric field at the output port (Fig. 5c)) about identical to the TE_{01} mode, imposing in input (Fig. 5 b)) an excitation with a single linear polarization of the TE_{11}.

3. Circular taper

A transition for the TE_{01} mode between the output radius (r1 = 1.48 mm) of the Serpentine Mode Converter and the input radius (r2 = 3 mm) of the TE_{01} to TE_{04} Mode Converter is studied comparing the results of three different type of taper: linear, exponential and cosine. For exponential and cosine profiles the CST-MS model is made using respectively the following analytical surfaces:

$$r(z) = r1 + \exp\left(\left(\frac{z}{L}\right) * \ln\left(\frac{r2}{r1}\right)\right) \tag{3}$$

$$r(z) = \left(\frac{r1 + r2}{2}\right) - \left(\frac{r2 - r1}{2}\right) * \cos\left(\pi * \frac{z}{L}\right) \tag{4}$$

Setting identical length of 20 mm for all the profiles with aluminum around the surface the best transmission of about 0.04 dB at f = 250 GHz is determined by means of CST-MS with a simple linear profile. The attenuation of the TE_{01} mode for the three cases is indicated in Fig. 6.

The reflection is lower than-35 dB for all the three circular tapers.

4. TE_{01}/TE_{04} rippled wall mode converter

Direct TE01 to TE04 conversion by rippled wall mode transformer in a oversized circular waveguide with average radius of r2 = 3 mm at a frequency around 250 GHz is studied in order to simplify the geometry using a single transition. Adopting a similar approach as in [10] to obtain an excellent conversion efficiency the wall deformation is given by:

$$r(z) = r2 * (1 + \sin\left(\Pi * \frac{z}{l}\right) * \left(e1 * \cos\left(2 * \Pi * \frac{z}{bc}\right) + e2 * \cos\left(2 * \Pi * \frac{z}{bc1}\right) + e3 * \sin\left(2 * \Pi * \frac{z}{bc2}\right)\right)) \tag{5}$$

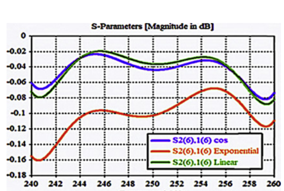

Fig. 6. Transmission of the mode TE_{01} for the three profiles.

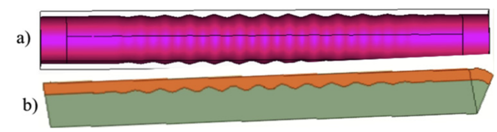

Fig. 7. Profile of the TE01/TE04 Rippled wall mode converter in a) CST-MS and b) HFSS model.

where e1 = 0.069 and bc = 2.93 mm, higher than the beat wavelength (λw) of 2.73 mm;

e2 = 0.01, bc1 = 15.75 mm, λw1 = 15.96 mm (TE_{01}/TE_{02} coupling);

e3 = 0.01, bc2 = 5.6 mm, λw2 = 5.76 mm (TE_{01}/TE_{03} coupling).

The amplitude of undesired modes, TE_{02} and TE_{03}, are limited by superposition of two additional terms to the main perturbation, corresponding to the beat wavelength between TE_{01} to TE_{02} and TE_{01} to TE_{03} respectively. In a circular waveguide with average radius of 3 mm the TE_{05} mode doesn't propagate at the frequency of 250 GHz and the correspondent TE_{01}/TE_{05} coupling term is not considered. The amplitude of the corrugation is multiplied by a term in *sin* to avoid a sharp discontinuity between the smooth circular waveguides and the corrugated converter. The models are represented in Fig. 7 a) and b) respectively for CST-MS and HFSS. In CST-MS inserting two symmetry planes along the longitudinal planes (xz and yz) with tangential electric field equal to 0, a limited number of propagation modes has been considered and the convergence is reached in a lower time. Using this boundary condition the order of the input mode becomes the second and 22^{th} is the order of the output modes. In HFSS splitting the structure three times along the longitudinal direction the whole volume is reduced at a quarter and the number of propagating modes becomes lower than 25, the maximum supported by HFSS. Two symmetry with a perfect electric field are set as boundary conditions along two longitudinal surfaces which delimits the volume. Now all the propagation modes are considered and the TE_{01} becomes the first mode while the TE_{04} is the 11^{th}. CST-MS provides excellent results with a S2(22),1(2) = -0.18 dB (97% efficiency) at f = 250 GHz including also the power losses.

A validation is carried out with HFSS and two other in house codes (mode matching and based on the theory of coupled mode) obtaining results in complete disagreement with CST_MS. In fact the maximum conversion is always centered at the operating frequency of 250 GHz but the level of -1 dB corresponds to an efficiency of only the 80%. Probably the CST-MS modeling using the previous complicated profile produces wrong values of S-parameters. In order to validate the results with all the codes a decision to simplify the corrugation has been taken considering only the main perturbation (e2 = e3 = 0). Finally choosing a period of bc = 2.88 mm and a corrugation of e1 = 0.074 for N = 16, the transmission coefficient versus the frequency plotted in Fig. 8 and calculated with all the four codes, is about identical in amplitude but translated in frequency. The maximum transmission of -0.16 dB

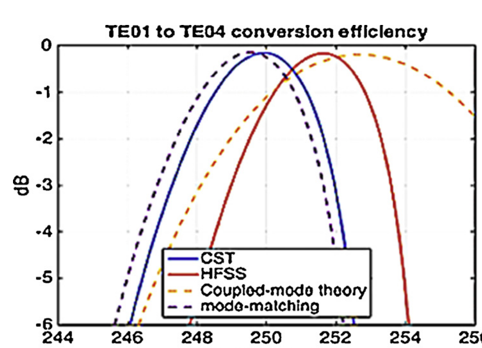

Fig. 8. TE01 to TE04 conversion efficiency deduced with two commercial codes and two in house codes.

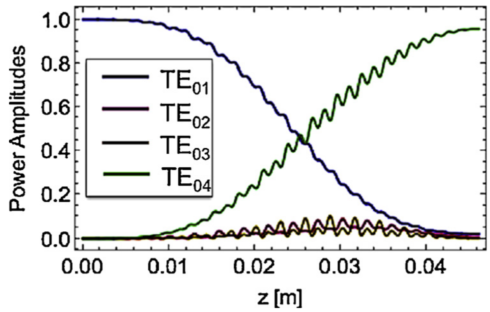

Fig. 9. Power amplitudes of the main modes as a function of z along the mode converter.

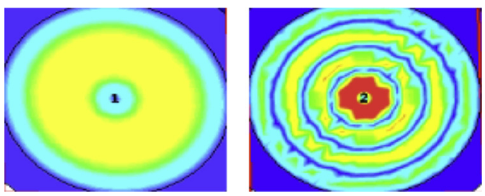

Fig. 10. Pattern of the electric field at the input port on the left and at the output port on the right.

corresponds to a frequency of 250 GHz for CST and slight lower for the mode matching. The frequency increases to 1518 GHz for HFSS and 252.2 GHz for the Coupled mode theory. The maximum difference in frequency compared to the operating frequency corresponds to a relative error of only the 0.8%.

The efficiency is the 97% including also the power losses and the overall length corresponds to 4518 mm. Considering the curve relative to the CST code the bandwidth (Δf), defined as the interval between frequencies with 90% of efficiency, is equal to 1.52 GHz. For a rippled wall mode converter Δf can be evaluated also by the following expression:

$$\eta = \eta o/(1 + \delta{*}\delta) \quad (6)$$

reported in [10] where $\delta = 2.6{*}\, N{*}(\Delta f/fo)$ for $N \geq 14$. Substituting f= = 250 GHz, N = 16, ηo = 0.97 and η = 0.9 the calculated value, slightly bigger, of 1.65 GHz is in good agreement with the CST-MS simulation results.

Only the TE_{04} mode is present in output as shown in Fig. 9 using the code based on the Coupled-mode theory.

The most dangerous spurious modes TE_{02} and TE_{03} have low amplitude in output. The CST representation of the electric field in Fig. 10 demonstrates that the mode transformation has been carried out successfully.

5. Conclusions

An optimization of the TE_{11}/TE_{04} Mode Converters for the Cold Test of a 250 GHz CARM Source has been successfully performed only using a linear taper and two mode converters with a less complicate geometry instead of three tapers and four mode converters designing a direct TE_{01} to TE_{04} transition in substitution of a step by step TE_{01} to $TE_{02,}$ TE_{02} to $TE_{03,}$ and TE_{03} to $TE_{04,}$ conversion. A first validation of the simulation tools at such a high frequency will be carried out through the construction of a short Bragg reflectors.

References

[1] E. Poli, et al., Electron-cyclotron-current-drive efficiency in DEMO plasmas, Nucl. Eng. 53 (2013) 013011.
[2] V.L. Bratman, et al., Relativistic gyrotrons and cyclotron autoresonance masers, Int. J. Elettron. 51 (1981) 541–567.
[3] F. Mirizzi, et al., A high frequency, high power CARM proposal for the DEMO ECRH system, Fusion Eng. Des. 96–97 (2015) 538–541, https://doi.org/10.1016/j.fusengdes.2015.02.026.
[4] E. Di Palma, et al., The CARM beam-wave interaction and cavity design, 10th Int. Workshop 2017 "Strong Microwave and Terahertz Waves: Source and Application", (2017).
[5] G.L. Ravera, S. Ceccuzzi, A. Doria, F. Mirizzi, I. Spassovsky, A.A. Tuccillo, Mode converters for the RF cold test of a 250 GHz CARM cavity, 45th European Microwave Conference (2015) 1180–1183.
[6] G.L. Ravera, et al., Mode converters in overmoded circular waveguide for a 250 GHz CARM source, Progress in the Electromagnetic Research Symposium (PIERS) (2017) 1211–1216.
[7] J.S. Levine, Rippled wall mode converter for circular waveguide, Int. J. Infrared Millimeter 5 (7) (1984) 937–951.
[8] W. Lawson, The design of serpentine-mode converter for high-power microwave applications, IEEE Trans. Microw. Theory Technol. 48 (May (5)) (2000) 809–814.
[9] S. Ceccuzzi, et al., Comparison of reflectors concepts for a 250 GHz CARM cavity, 10th Int. Workshop 2017 "Strong Microwave and Terahertz Waves: Source and Application", (2017).
[10] H. Kumric, et al., Optimization of mode converters for generating the fundamental TE01 mode grom the Gyrotron output at 140 GHz, Int. J. Infrared Millimeter 64 (1) (1988) 77–94.